JOURNAL OF MATERIALS SCIENCE 26 (1991) 2015–2022

1000 to 1300 K slow plastic compression properties of Al-deficient NiAl

J. D. WHITTENBERGER
NASA-Lewis Research Center, Cleveland, OH 44135, USA
K. S. KUMAR, S. K. MANNAN
Martin Marietta Laboratories, 1450 South Rolling Rd., Baltimore, MD 21227-3898, USA

Nickel aluminides containing 37, 38.5 and 40 at % Al have been fabricated by XD^{tm} synthesis and hot pressing. Such materials were compression tested in air under constant velocity conditions between 1000 and 1300 K. Examination of the microstructures of hot pressed and compression tested aluminides indicated that the structure consisted of two phases, γ' and NiAl, for essentially all conditions, where γ' was usually found on the NiAl grain boundaries. The stress–strain behaviour of all three intermetallics was similar where flow at a nominally constant stress occurred after about two plastic per cent deformation. Furthermore the 1000 to 1300 K flow stress–strain rate properties are nearly identical for these materials, and they are much lower than those for XD^{tm} processed Ni–50Al [1]. The overall deformation of the two phase nickel aluminides appears to be controlled by dislocation climb in NiAl rather than processes in γ'.

1. Introduction

Although the B2 cubic crystal structure intermetallic NiAl has many attractive features: for example a high melting point, relatively low density and oxidation resistance; the lack of low temperature toughness is one of the drawbacks inhibiting its use as a high temperature structural material. As martensite is known to form in Al-deficient nickel aluminide, and its formation is dependent on both composition and applied stress, it is possible that NiAl could be transformation toughened at room temperature by selecting an appropriate chemistry. Ideally energy would be dissipated by the martensitic reaction when material is deformed above its unstressed martensite start (M_s) temperature. Based on the work of Smialek and Hehemann [2] NiAl containing more than $\sim$ 38 at % Al should have M_s temperatures below 300 K; therefore such compositions would be candidates for transformation toughening.

Fracture toughness experiments [3] have been conducted on a series of XD^{tm} processed NiAl's containing 40, 38.5 and 37 Al (all compositions are in atom per cent unless noted), and the results indicate that it is possible to increase the room temperature toughness by fifty per cent. Since most proposed applications of NiAl are at elevated temperatures, it is then logical to evaluate the effect of low Al content on the high temperature mechanical properties. Such a study is particularly significant as the Ni–Al phase diagram (Fig. 1) indicates that nickel aluminides containing 37 to 40 atomic per cent Al are not thermodynamically stable at intermediate temperatures with decomposition into NiAl + Ni_3Al (γ') or even Ni_2Al and Ni_5Al_3 possible [5]. In general, however, these latter phases will not be seen as their formation requires prolonged exposure below $\sim$ 973 K [5]. At test temperatures between 1000 and 1300 K Ni–40Al should be a single phase while Ni–37Al would consist of NiAl + γ'. Ni–38.5Al, on the other hand, can possess both morphologies: NiAl above $\sim$ 1150 K and NiAl + γ' below this temperature. This paper presents data from 1000 to 1300 K slow compression testing of the above three compositions and compares these results with those for the single phase, equi-atomic NiAl.

2. Experimental procedure

The XD^{tm} process [6] was utilized to produce three different NiAl compositions which contained 37, 38.5 and 40 at % Al as determined by chemical analysis. After synthesis, the materials were compacted to full density by a combination of vacuum hot pressing at 20.7 MPa and 1725 K followed by hot isostatic pressing at 207 MPa and 1725 K. Two compacts of each composition were made in order to obtain sufficient specimens for testing. Right cylindrical compression specimens 12 mm long with a 5.5 mm diameter were prepared by electrodischarge machining and grinding where their length was parallel to the hot pressing direction. Constant velocity compression tests at speeds from 2.12×10^{-3} to 2.12×10^{-6} mm s^{-1} were conducted in a universal test machine to $\sim$ 8 per cent strain between 1000 and 1300 K in air. The autographically recorded load–time charts were converted to true compressive stresses, strains, and strain rates

0022–2461/91 $03.00 + .12

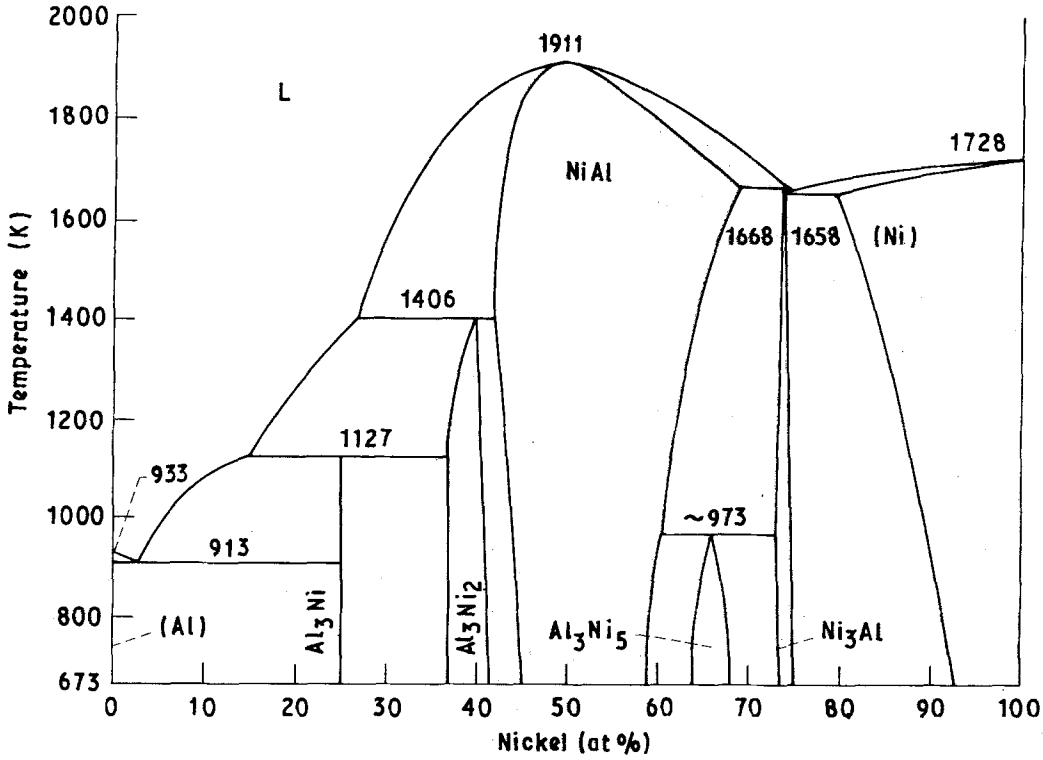

Figure 1 Ni–Al phase diagram [4].

via the offset method and the assumption of conservation of volume. Additional details regarding the test procedures can be found in [7].

Optical techniques were used to characterize the structure of selected as-received and compression tested samples. Grain sizes were determined by the circle intercept method after the microstructures had been revealed by immersion in a solution consisting of 25 ml HF and 75 ml H_2O which was saturated with molybdic acid. In general it was found that the presence of small amounts martensite and/or γ' were more readily detectable under differential interference lighting than bright light conditions.

3. Results

3.1. Materials

Typical photomicrographs of the hot pressed aluminides are presented in Fig. 2, and several clear differences among the three materials can be seen. Essentially all the grains in Ni–37Al (Fig. 2a) are outlined by γ', and many grains contain martensite laths. The grains for Ni–38.5Al (Fig. 2b) are partially ringed with γ'; however there was no indication of martensite. Although some evidence of γ' could be seen at higher magnifications, Fig. 2c reveals that the amount of γ' in Ni–40Al is small in comparison to the other two aluminides; furthermore martensite is absent. Additionally, as can be seen in Fig. 2, the grains tend to be elongated perpendicular to the hot pressing direction, and the grain size of Ni–37Al is somewhat larger than that for Ni–38.5Al or Ni–40Al (Table I). While not clearly visible at the current magnification, all three materials contain a dispersion of small Al_2O_3 particles which reside mainly on grain boundaries and are characteristic of XD^{tm} processed nickel aluminides [1].

3.2. Compression properties

3.2.1. Stress–Strain behaviour

Representative stress–strain diagrams obtained under different constant velocity conditions for the three aluminides are illustrated in Fig. 3. At 1000 K (Fig. 3a–c) testing at the fastest strain rate ($\sim 1.8 \times 10^{-4}\ s^{-1}$) resulted in yielding followed by strain softening which is pronounced in Ni–40Al (Fig. 3a) and much less so in the other two compositions (Fig. 3b, c). Deformation at slower strain rates generally lead to flow at a more or less constant stress after some initial strain hardening.

Based on the compositions and temperature range under investigation, the present materials should exhibit the greatest tendency to redistribute into two phases at 1000 K (Fig. 1). In an effort to determine if prior 1000 K exposure greatly influenced properties, specimens of each composition were aged for 100 h before testing at 1000 K and a strain rate of $1.8 \times 10^{-6}\ s^{-1}$. From these experiments, as indicated by the dashed curves in Fig. 3a–c, it is clear that there is little difference in behaviour between the aged and unaged specimens for Ni–40Al (Fig. 3a). Prior exposure sharply reduces the amount of work hardening for Ni–37Al (Fig. 3c) but seems to have essentially no effect on maximum strength. The behaviour of aged and unaged Ni–38.5Al samples (Fig. 3b) is similar to that of Ni–37Al; however, equivalency of strengths was obtained more quickly in Ni–38.5Al ($\sim$ 4% strain) than Ni–37Al ($\sim$ 8% strain).

Testing at 1100 and 1200 K yielded stress–strain curves similar to those shown in Fig. 3d–f for 1300 K deformation. Irrespective of composition steady state flow behaviour was observed after one or two per cent plastic deformation. Comparison of the data in Fig. 3 as a function of composition indicates that the flow

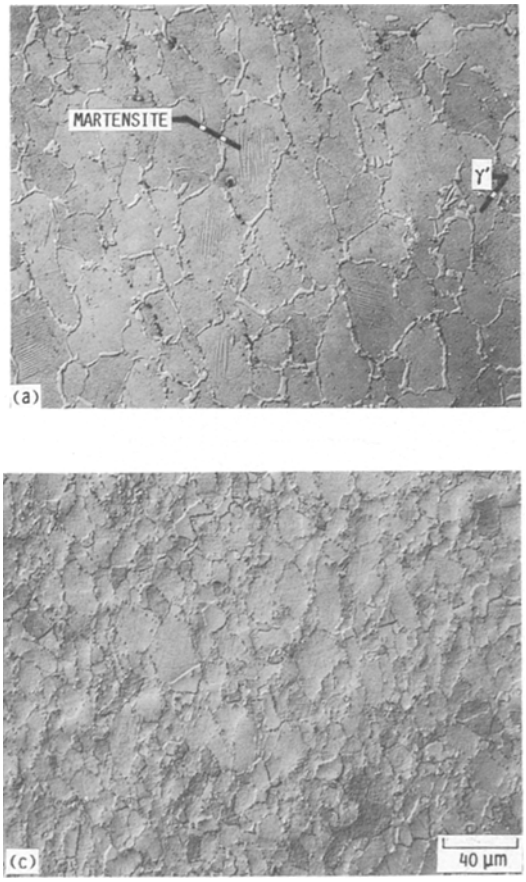

Figure 2 Microstructure of hot pressed XD^{tm} nickel aluminides. Hot pressing direction is horizontal. Specimens have been etched and photographed under differential interference contract (DIC) conditions; (a) Ni–37Al, (b) Ni–38.5Al and (c) Ni–40Al.

TABLE I Summary of grain size data for Al-deficient NiAl

Composition Al (at %)	Heat	As-fabricated	Grain diameter (μm) Tested at strain rate $\sim 1.8 \times 10^{-5}\,s^{-1}$ Temperature (K)			
			1000	1100	1200	1300
40	1	—	NT	NT	12	13
	2	8	8	8	9	NT
38.5	1	—	NT	NT	17	21
	2	12	12	12	15	NT
37	1	—	NT	NT	NT	18
	2	22	18	19	22	NT

NT = No samples tested.

strength does depend on Al content; however the dependency is not consistent over the range of temperatures and strain rates investigated. Furthermore the maximum differences in strength are generally small on an absolute scale: for example 7 MPa separates the strongest and weakest materials at 1300 K {tests at $1.8 \times 10^{-5}\,s^{-1}$} while at 1000 K Ni–37Al is ~ 30 MPa stronger than Ni–40Al {tests at $1.8 \times 10^{-6}\,s^{-1}$}.

3.2.2. Stress–strain rate behaviour

Fig. 4 presents the flow stress (σ)–strain rate ($\dot{\varepsilon}$) data for the three aluminides as a function of temperature where σ and $\dot{\varepsilon}$, with one exception, are average values from nominally constant flow regimes. For Ni–40Al tested at 1000 K and an approximate strain rate of $1.8 \times 10^{-4}\,s^{-1}$, σ and $\dot{\varepsilon}$ are means calculated over the diffuse yield point. At 1000 K the data for specimens subjected to the 100 h annealing at 1000 K prior to testing are shown as half filled circles, while the two pressings (heats) of each aluminide composition are represented through the use of filled (first heat) and open (second heat) symbols.

The strain rate data in Fig. 4 were fitted to the standard power law and temperature compensated power law rate expressions

$$\dot{\varepsilon} = A\sigma^n \quad (1)$$

$$\dot{\varepsilon} = B\sigma^n \exp(-Q/RT) \quad (2)$$

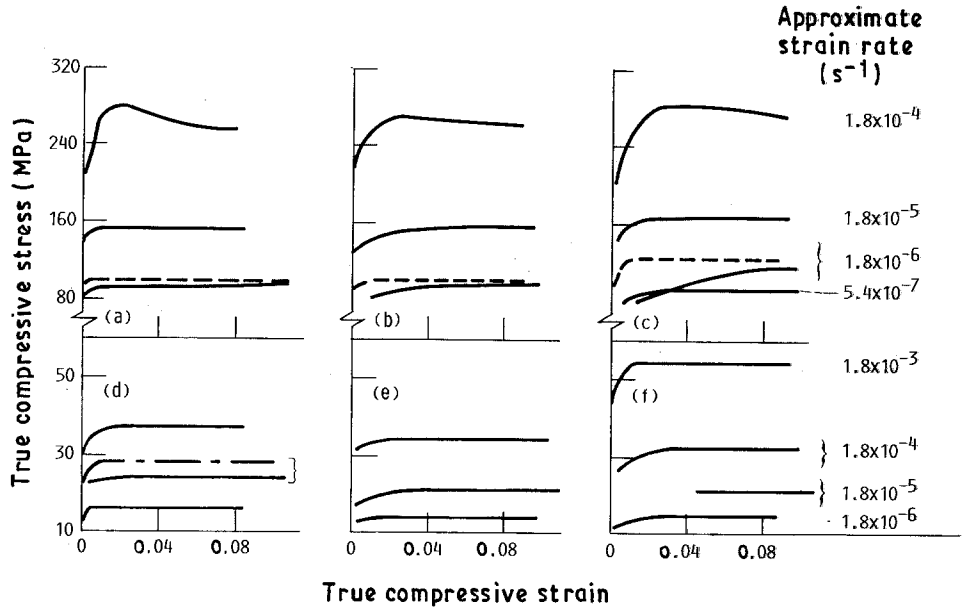

Figure 3 True compressive stress–strain diagrams as a function of strain rate for Ni–40Al (a, d), Ni–38.5Al (b, e) and Ni–37Al (c, f) tested at 1000 K (parts a–c) and 1300 K (parts d–f).

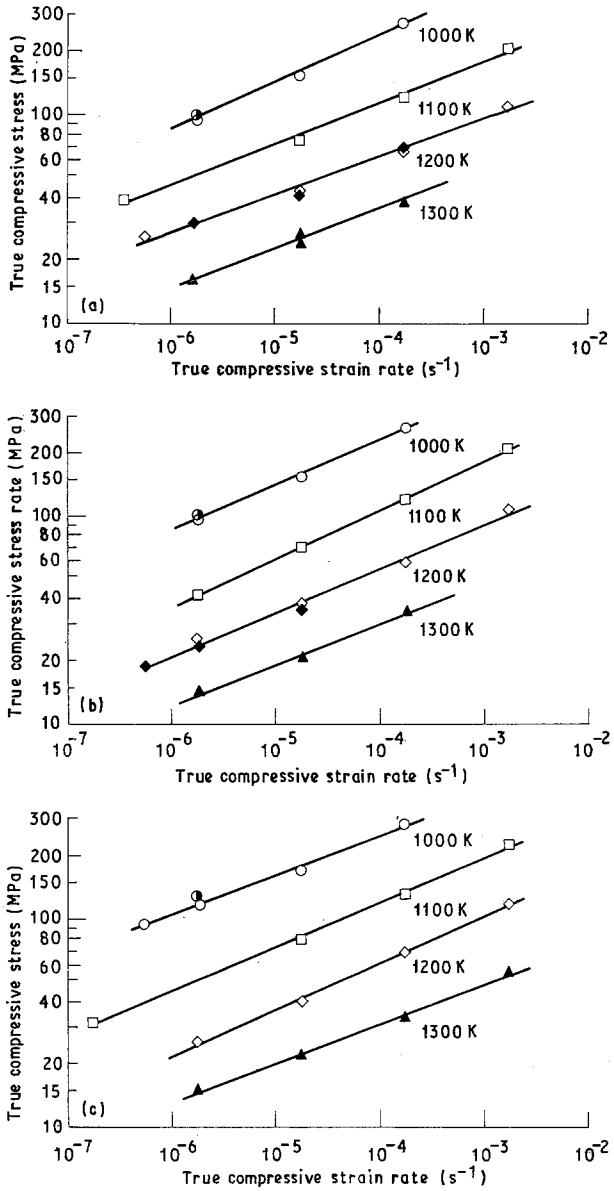

Figure 4 True compressive flow stress–strain rate behaviour for (a) Ni–40Al, (b) Ni–38.5Al and (c) Ni–37Al tested between 1000 and 1300 K.

where A and B are constants, n is the stress exponent, Q is the activation energy for creep, R is the gas constant and T is the absolute temperature. Fits were accomplished by linear regression techniques, and the results of these calculations including the Coefficients of Determination R_d^2 are given in Table II. The influence of heat of material was checked by the use of a

TABLE II Power law and temperature compensated–power law fits of true compressive flow stress–strain rate data for Al–deficient NiAl.

(a) *Power Law fits*

Composition (% Al)	Temperature (K)	A (s^{-1})	n	R_d^2
40	1000	3.13×10^{-15}	4.4	0.995
	1100	3.62×10^{-15}	5.08	0.996
	1200	1.11×10^{-14}	5.55	0.985
	1300	1.02×10^{-12}	5.16	0.954
38.5	1000	8.98×10^{-16}	4.67	0.997
	1100	2.61×10^{-13}	4.24	1.00
	1200	5.47×10^{-13}	4.74	0.99
	1300	2.27×10^{-12}	5.17	0.994
37	1000	1.17×10^{-17}	5.40	0.987
	1100	1.90×10^{-14}	4.69	0.998
	1200	1.11×10^{-12}	4.45	0.997
	1300	1.34×10^{-12}	5.29	0.994
50[a]	1200	1.28×10^{-17}	6.74	1.00
	1300	3.89×10^{-15}	5.90	0.998

(b) *Temperature compensated-power law fits*

Composition (% Al)	Temperature (K)	B (s^{-1})	n	Q (kJ mol^{-1})	R_{d^2}
40	1000–1300	26.7	5.07	333.1	0.978
38.5	1000–1300	248	4.62	331.7	0.991
37	1000–1300	3380	4.80	367.5	0.989
All	1000–1300	267	4.77	341.4	0.969
50[a]	1200–1300	0.0336	5.94	324.5	0.998

[a] Ref. [1]

dummy variable with Equations 1 and 2, and no statistically significant effect was found in either power law or temperature compensated-power law descriptions. In view of the high R_d^2's (Table II), power laws adequately describe the 1000 to 1300 K compressive flow stress–strain rate properties for all three materials.

Comparison of the strengths of the Al–deficient materials indicates that Ni–38.5Al (Fig. 4b) tends to be slightly weaker than either Ni–40Al (Fig. 4a) or Ni–37Al (Fig. 4c). While this behaviour is best reflected in the 1200 K data, it can also be seen that differences in strength are quite small for the three aluminides over the investigated strain rate–temperature range. In fact a regression fit of all the data to Equation 2 yielded a reasonable stress exponent and activation energy (4.77, 341 kJ mol^{-1}) with the respectable R_d^2 of 0.97 (Table II); furthermore statistical testing revealed that composition was not a significant variable.

3.3. Post test microstructures

Examples of the microstructures observed following testing are given in Figs 5 and 6. After deformation at 1000 K the NiAl grains in both Ni–37Al (Fig. 5a) and Ni–38.5Al (Fig. 5b) are completely outlined with γ' while little γ' is visible in Ni–40Al (Fig. 5c). Significant amounts of γ' were also found in the two most Al–deficient aluminides after 1300 K compression (Fig. 6a, b); however the grains were not completely ringed with the second phase. No γ' could be found in the Ni–40Al sample tested at 1300 K (Fig. 6c).

Ni–37Al tested at 1100 K possessed grains which were entirely bordered by γ', while only incomplete γ' rings were formed at 1200 K. After 1100 K testing the grains of Ni–38.5Al were partly outlined with γ', and this type of microstructure was also observed following 1200 K deformation. Although some γ' was found after either 1100 or 1200 K testing of Ni-40Al, the number, size and amount of γ' particles were small (Fig. 7). Fig. 7 also illustrates the presence of small Al_2O_3 particles (bright spots) usually found on the grain boundaries of powder processed XD^{tm} aluminides. Qualitatively for Ni–37Al and Ni–38.5Al the amount of γ' decreased as Al content and/or temperature increased. Lastly grain size measurements as a function of temperature on specimens tested at strain rates of $\sim 2 \times 10^{-5}$ s^{-1} indicated that the microstructures were resistant to grain growth (Table I).

4. Discussion

4.1. Phase equilibrium

Some disagreement seems to exist among the compositions of the three Al–deficient aluminides and the Ni–Al phase diagram (Fig. 1). Assuming a rapid quench to room temperature, Fig. 1 predicts that γ' should be absent from Ni–40Al tested between 1000 to 1300 K and from Ni–38.5Al tested above $\sim$ 1150 K. As can be seen in Fig. 7 for Ni–40Al and Fig. 6b for Ni–38.5Al, this is not the case. We believe that these discrepancies are due to the difficulty in resolutionizing the γ' which precipitated following hot isostatic pressing. In other work [8] involving the effect of heat treatment on the microstructure of the low Al

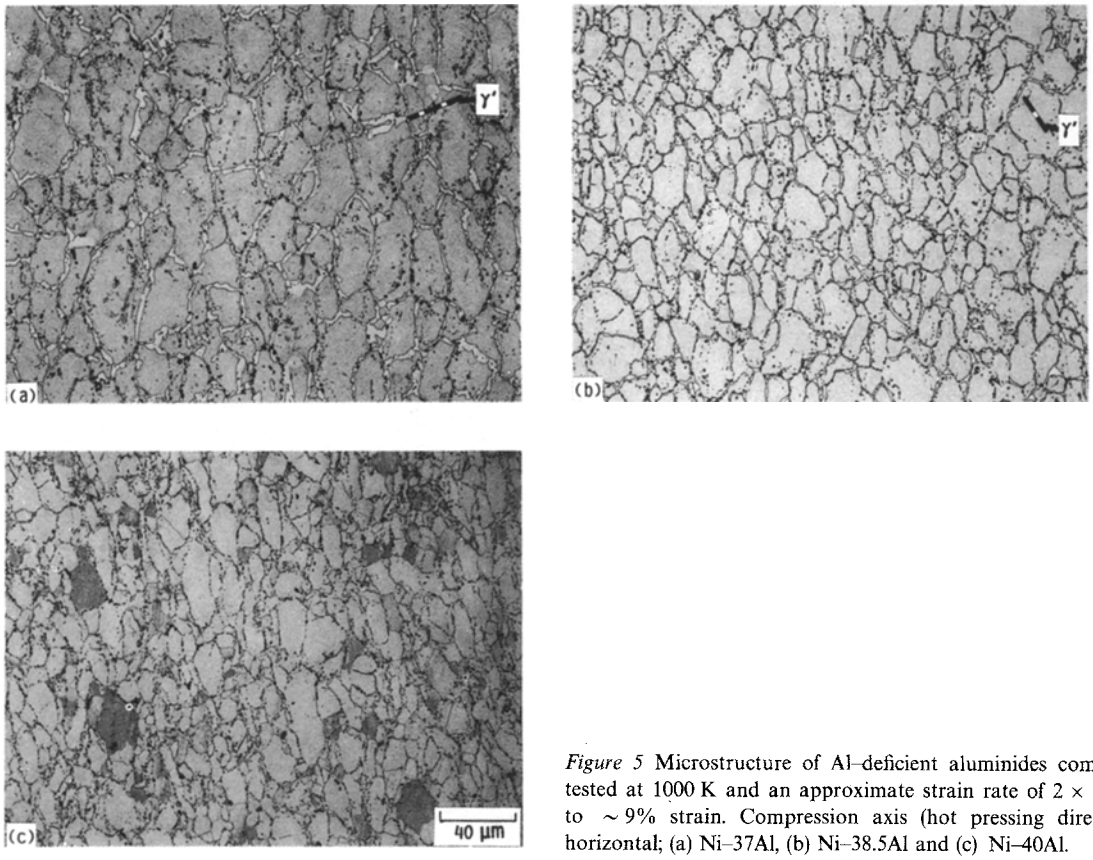

Figure 5 Microstructure of Al–deficient aluminides compression tested at 1000 K and an approximate strain rate of 2×10^{-5} s^{-1} to $\sim$ 9% strain. Compression axis (hot pressing direction) is horizontal; (a) Ni–37Al, (b) Ni–38.5Al and (c) Ni–40Al.

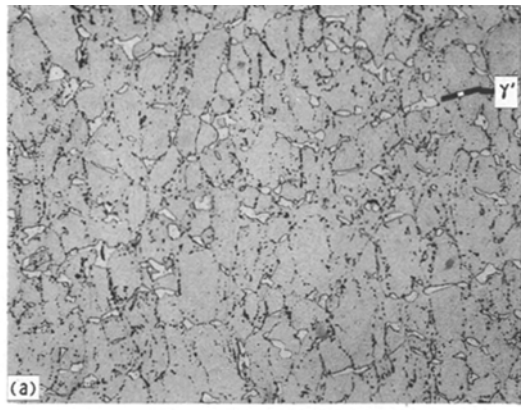

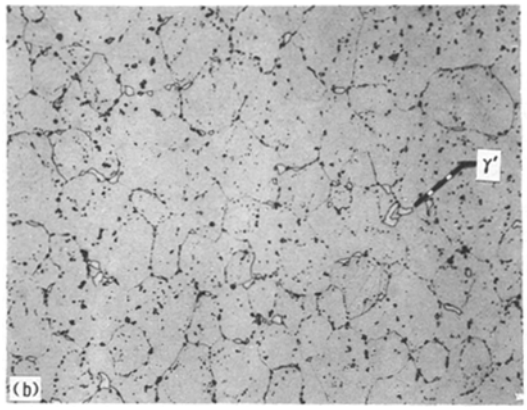

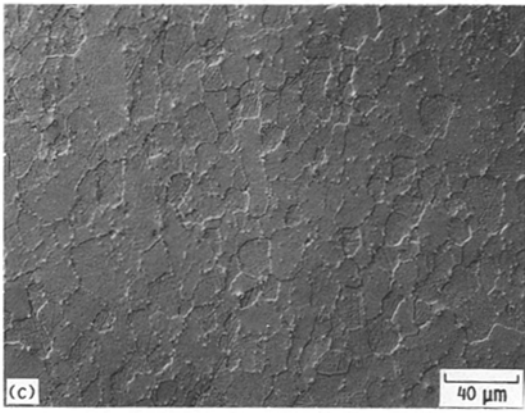

Figure 6 Microstructure of Al-deficient aluminides compression tested at 1300 K and an approximate strain rate of $2 \times 10^{-5} s^{-1}$ to ~ 10.5% strain. Compression axis (hot pressing direction) is horizontal; (a) Ni–37Al, (b) Ni–38.5Al and (c) Ni–40Al under DIC conditions.

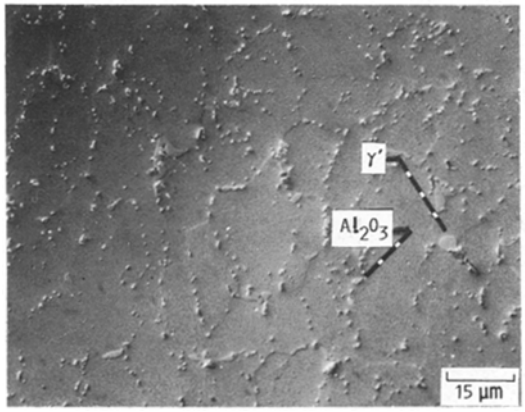

Figure 7 Microstructure of Ni–40Al compressed at 1200 K and an approximate strain rate of $2 \times 10^{-5} s^{-1}$ to 9% strain. Compression axis (hot pressing direction) is horizontal; DIC conditions.

materials, it was noted that isothermal exposures at ~ 1650 K for 4 h were required for complete solution treatment.

4.2. Mechanical properties

4.2.1. Comparison to Ni–50Al

The compressive flow strength–strain rate behaviour of the Al-deficient aluminides is compared to those for Ni–50Al in Fig. 8. These data are limited to 1200 and 1300 K in order to contrast XD^{tm} processed materials with similar grain sizes and second phase (Al_2O_3) content. First, this figure illustrates the near equivalence in strength among Ni–37Al, Ni–38.5Al and Ni–40Al at these test temperatures. Secondly, it is quite clear that the Ni–50Al is significantly stronger than the low Al versions; for instance Ni–50Al tested at 1300 K is as strong as NiAl containing 37–40% Al tested at 1200 K. While such a difference in strength is technologically important, this behaviour is probably the simple reflection of unequal homologous temperatures among the compositions. For example utilizing the solidus temperature as the melting point for the Al-deficient aluminides, 1200 K testing takes place at homologous temperatures ranging from 0.67 (Ni–40Al) to 0.685 (Ni–37Al). This range is quite comparable to the value of 0.68 for Ni–50Al tested at 1300 K.

In terms of power law and temperature compensated power law descriptions (Table II), the difference in strength due to relative Al levels is reflected in the pre-exponential constant(s) and stress exponents rather than the activation energy(s). For example with the temperature compensated power law formulation (Equation 2), Ni–50Al has a much lower constant than the Al-deficient materials (0.0336 versus 27–3380), and the stress exponent of Ni–50Al is about one unit higher (5.9 versus 4.7–5.1) while the activation energies are nearly identical (325 versus 332–368 kJ mol^{-1}).

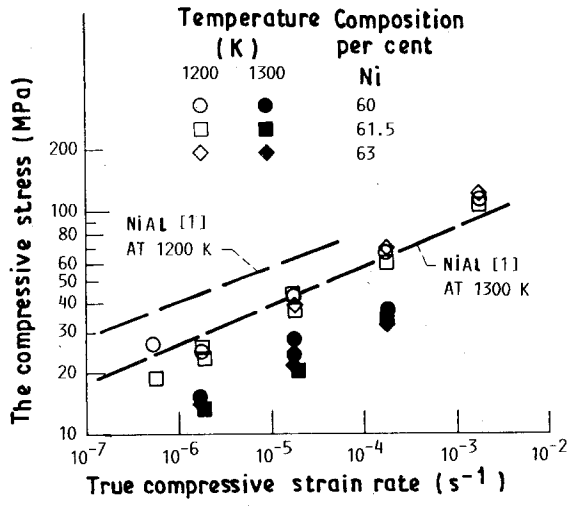

Figure 8 Comparison of the 1200 and 1300 K flow strength–strain rate properties of XD^{tm} processed nickel aluminides.

4.2.2. Deformation mechanisms

Based on the calculated activation energies alone, little can be decided about the thermally activated process(es) controlling deformation in the Al-deficient materials. Previous measurements [9, 10] of high temperature activation energy for creep in γ' have yielded values on the order of 320 kJ mol^{-1} for both polycrystalline and single crystal forms: while slow plastic compressive flow experiments on single phase, polycrystalline NiAl have yielded activation energies of 325 kJ mol^{-1} for XD^{tm} processed Ni–50Al [1] and 314 kJ mol^{-1} for extruded aluminides [11] containing from 45.5 to 51.6 at % Al. The similarity of these activation energies with those measured for the three low Al materials precluded specific assignment of the thermally controlling process to either of the two phases.

In terms of dislocation mechanisms γ' deforms by a viscous glide as evidenced by a stress exponent on the order of 3–3.5 [9, 12, 13]. NiAl, on the other hand, is controlled by a dislocation climb process involving the formation of subgrains which leads to stress exponents of about 5.5–6 [1, 11]. These types of behaviour can, however, be subverted by several factors. For example, if the grain size of NiAl is smaller than the equilibrium subgrain size, strengthening can occur, and the stress exponent should approach 8 [11, 14, 15]. However based on analysis of the current materials (Appendix), grain size strengthening does not appear to be taking place in the current Al-deficient NiAl's.

At elevated temperatures small grain sizes can also have the opposite effect, and weakening through diffusion creep mechanisms take place. Such phenomena have been apparently seen in both γ' [10] and NiAl [11, 14]. The work by Schneibel *et al.* [10] on a $\sim$ 55 μm grain size Ni–23.5Al–0.5 Hf–0.2B γ' alloy is particularly interesting in that they report that diffusion creep occurs at 1033 K and low stresses (< 10 MPa). In view of the current test temperatures and certainty that the grain size of γ' in the Al-deficient materials (Figs 2, 5, 6 and 7) are at least one order of magnitude smaller than the grain size determined by Schneibel *et al.* [10], it is probable that diffusional creep makes a significant contribution to the straining of γ' at and above 1000 K with the γ' NiAl interfaces providing the necessary vacancy sinks and sources. In view of the possibility of diffusional creep in γ' and the apparent independence of strength on the amount of γ', it is unlikely that deformation process(es) in γ' are the rate controlling mechanism in the two phase γ' + NiAl intermetallics. Vaandrager and Pharr [16] have studied the creep of alpha brass containing a boundary phase (Pb) as a function of temperature, and they found that the creep mechanism and stress exponent remained constant even when the second phase was molten. Furthermore it appeared that deformation of leaded brass was identical to that of pure α–brass. Perhaps the Al-deficient NiAl's behave in a similar manner, where the γ' is in effect liquid like (flows by a viscous mechanism) and plays no role in the overall deformation of these materials. Therefore the measured stress exponent of about 5 (Table II) indicate that dislocation climb in the NiAl grains is probably the rate controlling process in nickel aluminides containing from 37–40 at % Al and tested between 1000 and 1300 K.

5. Conclusions

XD^{tm} processed nickel aluminides containing 37, 38.5 and 40 at % Al were compression tested between 1000 and 1300 K. The stress–strain–strain rate properties were nearly identical for all three materials, and the strengths were much lower than those for XD^{tm} processed Ni–50Al. While the microstructures of hot pressed and compression tested aluminides indicated that they generally consisted of γ' and NiAl, deformation appears to be controlled by dislocation climb in NiAl rather than processes in γ'.

Appendix

Examination for grain size strengthening effects

Although no quantitative data exists on the size of subgrains formed in NiAl, the recent review and analysis of subgrain diameter–stress relationships by Raj and Pharr [17] indicates that the average subgrain size d_s can be estimated to within a factor of two from

$$d_s = \frac{23bG}{\sigma} \qquad \text{(A1)}$$

where b is the magnitude of the Burgers vector and G is the shear modulus. Values of the estimated subgrain size are tabulated as a function of stress in Table AI. For all practical purpose they are independent of temperature since the elastic modulus (2.6G) for NiAl only varies $\sim$ 15 GPa between 1000 and 1300 K [18].

As Ni–40Al has the smallest grain size (Table I), it is the most likely material to exhibit strengthening due to a limitation on the subgrain diameter. Based on Equation (A1) grain size strengthening should be seen when the flow stress is less than $\sim$ 50 MPa; comparison of this value with Fig. 4a indicates that grain size effects could be possible at 1300 K and perhaps the low strain rate regime ($\dot{\varepsilon} < 5 \times 10^{-5}$ s^{-1}) at 1200 K. Within the limits of the present data, neither obvious curvature of the flow strength–strain rate plot is occurring at 1200 K (Fig. 4a) nor does the stress exponent for the 1300 K experiments appear to be higher than those for lower temperature tests (Table IIa). This behaviour, coupled with the factor of two

TABLE AI. Estimated[a] subgrain diameters in NiAl.

Stress (MPa)	d_s μm	Stress (MPa)	d_s μm
300	2	10	60
120	5	7.5	80
60	10	6	100
30	20	2	300
15	40		

[a] $b = 2.9 \times 10^{-4}$ μm, $G = E/2.6$ where Young's modulus data E from [18]

limitation on calculated quantities *via* Equation (A1), indicates that grain size hardening probably does not take place in the present Al–deficient intermetallics.

Acknowledgement

JDW would like to acknowledge M. V. Nathal for pointing out that the difference in strength between the Al–deficient aluminides and Ni–50Al could be due to a homologous temperature effect.

References

1. J. D. WHITTENBERGER, R. K. VISWANADHAM, S. K. MANNAN and B. SPRISSLER, *J. Mater. Sci.* **25** (1990) 35.
2. J. L. SMIALEK and R. F. HEHEMANN, *Met. Trans.* **4** (1973) 1571.
3. K. S. KUMAR and S. K. MANNAN, Martin Marietta Progress Report MML TR 88-66c, Aug. 1988.
4. M. F. SINGLETON, J. L. MURRAY and P. NASH, in "Binary Alloy Phase Diagrams, Vol. 1, edited by T. H. Massalski, J. L. Murray, L. H. Bennett and H. Baker (ASM, Metals Park, OH, 1986) p. 140.
5. P. S. KHADKIHAR, I. E. LOCCI and K. VEDULA, Unpublished research.
6. A. R. C. WESTWOOD, *Met. Trans. A* **19A** (1988) 749.
7. J. D. WHITTENBERGER, *Mater. Sci. Eng.* **57** (1983) 77.
8. K. S. KUMAR, S. K. MANNAN and S. A. BROWN, Unpublished research.
9. D. P. POPE and S. S. EZZ, *Int. Metals Rev.* **29** (1984) 136.
10. J. H. SCHNEIBEL, G. F. PETERSEN and C. T. LIU, *J. Mater. Res.* **1** (1986) 68.
11. J. D. WHITTENBERGER, *J. Mater. Sci.* **22** (1987) 394.
12. D. M. SHAH, *Scripta Met.* **17** (1983) 997.
13. M. V. NATHAL, J. O. DIAZ and R. V. MINER, in High-Temperature, Ordered Intermetallic Alloys III, Proc. Mat. Res. Soc. Symp., Vol 133, edited by N. S. Stoloff, C. C. Koch, C. T. Lui and A. I. Taub (MRS, Pittsburgh, PA, 1989) pp. 269.
14. J. D. WHITTENBERGER, *J. Mater. Sci.* **23** (1988) 235.
15. J. D. WHITTENBERGER, NASA TM 101382, 1988.
16. B. L. VAANDRAGER and G. M. PHARR, *Scripta Metall.* **18** (1984) 1337.
17. S. V. RAJ and G. M. PHARR, *Mater. Sci. Eng.* **81** (1986) 217.
18. M. R. HARMOUCHE and A. WOLFENDEN, *J. Test. Eval.* **15** (1987) 101.

Received 31 July 1989
and accepted 19 February 1990